Organic Electronics 54 (2018) 89–93

Contents lists available at ScienceDirect

Organic Electronics

journal homepage: www.elsevier.com/locate/orgel

Inelastic electronic resonant transport in single-molecule devices

Bo-Lin Li[a,b], Yexin Feng[a], Ke-Qiu Chen[a,*]

[a] Department of Applied Physics, School of Physics and Electronics, Hunan University, Changsha, 410082, China
[b] Chongqing Key Laboratory of Extraordinary Bond Engineering and Advanced Materials Technology (EBEAM), Yangtze Normal University, Chongqing, 408100, China

ARTICLE INFO

Keywords:
Single-molecule device
Current-voltage curve
Current plateau
Temperature
Inelastic resonant tunneling

ABSTRACT

In this study, the integral expression of inelastic transport, which combined with nonequilibrium Green's function and density functional theory, is extended to investigate the inelastic electrical transport properties of single-molecule device. Results show that the height of the current plateau will increase along with the temperature. It is found that this increase in the height of the current plateau is caused by inelastic resonant tunneling rather than the decoherence mechanism of the quantum interference effect. And we find that some small steps and the tilt in the main current plateau are also responsible by the inelastic processes. These results help us to understand the electrical transport mechanisms in single-molecule devices.

1. Introduction

Single-molecule devices have a broad range of applications in future logical, sensing and energy-harvesting devices [1–5]. Such as all the logical functions of traditional semiconductors can be reproduced using single-molecule devices, including rectification [6–11], field effect [12,13], negative differential resistance [14–18], spin filtration [19–22] and giant magnetoresistance effects [23–26]. A deep understanding of the mechanisms underpinning the operation of single-molecule devices is therefore important for the design and production of single-molecule devices. In addition to the elastic transport properties of single-molecule devices being studied, the effects of electron-phonon interactions (EPIs) have also recently attracted considerable attention [27–31]. EPI effects such as vibrational excited states [32,33], inelastic cotunneling [34], Franck-Condon blockade [35,36], and vibration-induced decoherence of the quantum interference effect [27–29] have been reported in single-molecule devices. Our previous studies have also predicted that the spin filtration, giant magnetoresistance, and spin-dependent Seebeck effects in graphene nanoribbons may be significantly affected by EPIs [31,37,38]. All of these important effects indicate that we should pay more attention to the EPIs in single-molecule devices.

The current-voltage curves in nanoscale electronic devices usually exhibit step-like plateaus when operated in a low temperature environment [28,32,39,40]. Those plateaus can usually be explained using elastic transport theory as follows: for a device with separate resonant tunneling channels, a resonant tunneling channel can contribute to the electrical current only when it is included in the bias window. Thus, once a channel is included in the bias window, the current will be constant (i.e., form a plateau) even when the bias is increased until another channel is included in the bias window. Recently, Ballmann et al. measured the electrical currents of several single-molecule devices using the mechanically controlled break junction technique [28]. They discovered that the height of the current plateau increases along with the temperatures in some single-molecule devices. It should be noted that elastic transport theory cannot explain this kind of increase. Thus, the only way to understand it is to take the influence of phonons into account. In Ref. [28] this phenomenon is therefore explained via the vibration-induced decoherence of the quantum interference effect. However, Ref. [28] does not present a detailed theoretical calculation for how exactly this decoherence mechanism affects the results. Here, we have therefore used density functional theory (DFT) and the nonequilibrium Green's function (NEGF) method to address this gap in the literature. The results from our theoretical calculations are in agreement with the experimental results and indicate that the increase in the height of the current plateau may not be based on the quantum interference and decoherence mechanism, but on inelastic resonant tunneling.

2. Methods

As is usual as in the lowest order expansion method [41,42], we calculated the elastic and inelastic transport currents I_{el} and I_{in} separately, and then summed to determine the total current I ($I = I_{el} + I_{in}$). The elastic current is described by the Landauer formula [43–46] as follows:

* Corresponding author.
E-mail address: keqiuchen@hnu.edu.cn (K.-Q. Chen).

https://doi.org/10.1016/j.orgel.2017.12.019
Received 21 October 2017; Received in revised form 3 December 2017; Accepted 16 December 2017
Available online 20 December 2017
1566-1199/

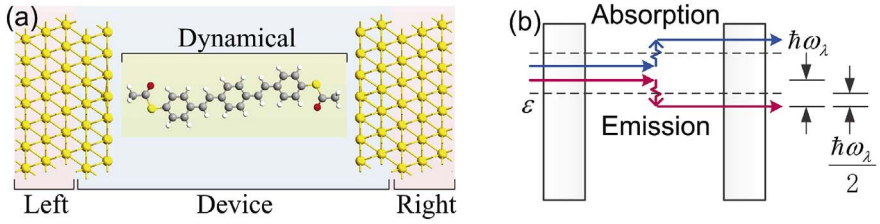

Fig. 1. (a) The schematic structure of the single-molecule device, which is set up as dynamical, device, and left (or right) electrode regions; only the couplings to the local phonons in the dynamical region are considered. The periodic supercell of the electrodes was taken to be 4×4 Au(111) surfaces. (b) Schematic of the inelastic transport processes from the left to the right electrode. In our method, see Eqs. (3) and (4), the energy variable ε lies at the median level of the energy of the incoming and outgoing states of the two electrodes (dashed lines in the figure).

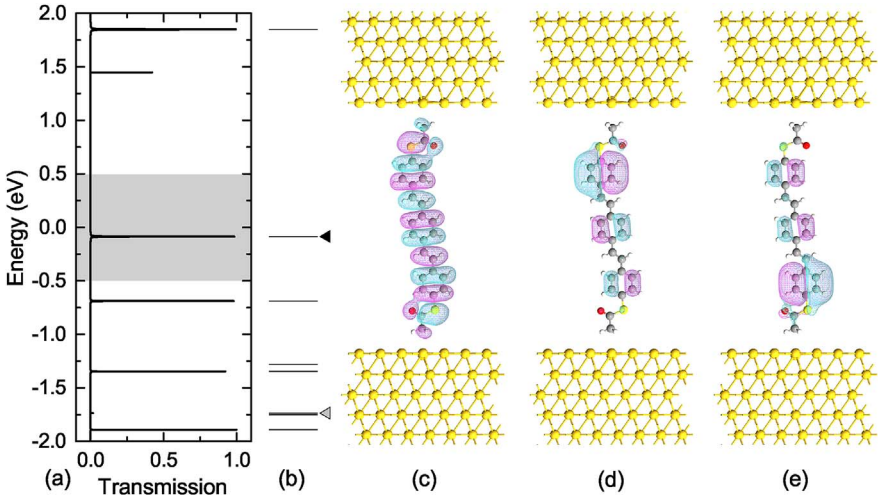

Fig. 2. (a) The elastic transmission of the single-molecule device. The shaded region shows the energy window for the largest bias (1V) considered here. (b) The molecular energy spectra of the central molecule. (c)–(e) The molecular projected self-consistent Hamiltonian of the molecular orbital states of the molecule, where (c) shows the highest occupied molecular orbital (HOMO) at energy level near -83.5 me V, marked by the solid triangle in (b), and (d) and (e) are the two energy levels that display quantum interference with each other; their energy levels are located near -1.737 eV, marked by the grey triangle in (b), and the energy difference between those two states was $\Delta E = 0.46$ m eV.

$$I_{\rm el} = \frac{G_0}{e}\int d\varepsilon [f(\varepsilon-\mu_{\rm L}) - f(\varepsilon-\mu_{\rm R})]\mathscr{T}(\varepsilon), \tag{1}$$

where $G_0 = 2e^2/h$ is the conductance quantum, $f(\varepsilon)$ is the Fermi-Dirac function, and μ_L and μ_R are the chemical potentials of the left and right electrodes, respectively. For a positive external bias V_b, we set $\mu_{L/R} = \pm eV_b/2$. The transmission coefficient is given by $\mathscr{T}(\varepsilon) = {\rm Tr}[\mathbf{G}^r\Gamma_L\mathbf{G}^a\Gamma_R]$, where $\mathbf{G}^{r,a}$ is the unperturbed (noninteracting with phonons) retarded/advanced device Green's function, and $\Gamma_{\alpha=L,R}$ is the broadening of the states inside the device region caused by coupling to the left/right electrode.

If we only take the inelastic transport processes of the first-order Born scattering processes [31,47], which are represented by arrows in Fig. 1(b), into consideration, we can write the inelastic current in integral expression [37,48].

$$I_{\rm in} = \frac{G_0}{e}\sum_\lambda \int d\varepsilon(\gamma_{{\rm em},\lambda}\mathcal{F}_{{\rm em},\lambda} + \gamma_{{\rm abs},\lambda}\mathcal{F}_{{\rm abs},\lambda}), \tag{2}$$

where

$$\gamma_{{\rm em},\lambda} = {\rm Tr}[\mathbf{M}_\lambda\widetilde{\mathbf{A}}_L(\varepsilon'_+)\mathbf{M}_\lambda\mathbf{A}_R(\varepsilon'_-)], \tag{3}$$

$$\gamma_{{\rm abs},\lambda} = {\rm Tr}[\mathbf{M}_\lambda\widetilde{\mathbf{A}}_L(\varepsilon'_-)\mathbf{M}_\lambda\mathbf{A}_R(\varepsilon'_+)], \tag{4}$$

$$\mathcal{F}_{{\rm em},\lambda} = f_L(\varepsilon'_+)(1-f_R(\varepsilon'_-)+N_\lambda) - N_\lambda f_R(\varepsilon'_-), \tag{5}$$

$$\mathcal{F}_{{\rm abs},\lambda} = N_\lambda f_L(\varepsilon'_-) - f_R(\varepsilon'_+)(1-f_L(\varepsilon'_-)+N_\lambda), \tag{6}$$

and where $\varepsilon'_\pm$ denotes $\varepsilon \pm 1/2\hbar\omega_\lambda$, λ is the index of phonon, $\mathbf{M}_\lambda$ is the electron-phonon coupling matrix, $\mathbf{A}_\alpha = \mathbf{G}^r\Gamma_\alpha\mathbf{G}^a$ and its time-reversed version $\widetilde{\mathbf{A}}_\alpha = \mathbf{G}^a\Gamma_\alpha\mathbf{G}^r$ are the spectral density matrices, and f_α and N_λ are the Fermi-Dirac and Bose-Einstein distribution functions, respectively.

Here, $\gamma_{{\rm em/abs},\lambda}$ represents the patency rate of the phonon emission/absorption process, which is indicated by the red/blue arrows in Fig. 1(b). More specifically, $\gamma_{{\rm em},\lambda}(\varepsilon)$ is the patency rate of the first-order Born scattering process from the left state $|\psi_l(\varepsilon + 1/2\hbar\omega_\lambda)\rangle$ to the right state $|\psi_r(\varepsilon - 1/2\hbar\omega_\lambda)\rangle$, while $\gamma_{{\rm abs},\lambda}(\varepsilon)$ is the patency rate from the state $|\psi_l(\varepsilon - 1/2\hbar\omega_\lambda)\rangle$ to the state $|\psi_r(\varepsilon + 1/2\hbar\omega_\lambda)\rangle$.

To compare our calculation results with the experimental results in Ref. [28], we modeled our device to be like the one shown in Fig. 1(a). In it a 1,4-bis[4'-(acetylthio)styryl]benzene [49] molecule is connected to two Au(111) surfaces. We only considered the local vibrations of this molecule, and the coupling between these vibrations and the electronic Hamiltonian inside the central device region. The electronic and vibrational Hamiltonian, electron-phonon coupling matrices $\mathbf{M}$, the transmission $\mathscr{T}(\varepsilon)$ and the trace given $\gamma_{\rm em/abs}(\varepsilon)$ were calculated using NEGF-DFT codes in the Atomistix ToolKit [41,42,46,50,51] under equilibrium conditions. The DFT calculations were performed using the generalized gradient approximation [52] exchange-correlation functional, single-ζ polarized basis set for the Au atoms and double-ζ polarized basis set for the C, H, O and S atoms, while the cut-off energy was at 400 Ry. The structure in the device region was relaxed until the forces acting on the atoms dropped below 0.02 eV/Å. The interval between points on the energy grid was 0.25 meV for the calculation of the elastic transmission and inelastic γ functions. Owing to DFT's low accuracy for describing extremely low-energy phonons, the influence of phonons which energies below 3 meV were ignored when calculating the current.

3. Results and discussions

First, we investigated the elastic transport properties of the 1,4-bis[4'-(acetylthio)styryl]benzene single-molecule device. The elastic transmission of this device and the molecular energy spectrum of the central molecule are presented in Fig. 2(a) and (b), respectively. In the figure, the maximum transmission energy window (bias window) for $V_b = 1$V is indicated by the shaded area, which indicates the region in which the transmission will contribute to the currents. It is obvious that only the molecular energy level at 86.5 m eV, i.e., the highest occupied molecular orbital (HOMO), is effective when the bias is limited to $|V_b| \le 1$V. From this molecular energy spectrum and from the transmission results, we could easily obtain the characteristic step-like elastic current-voltage (*I-V*) curves (see Fig. 3(a)). Note that these elastic current curves have a similar shape to the experimentally